Journal of Hepatocellular Carcinoma Dovepress

Open Access Full Text Article ORIGINAL RESEARCH

Oxymatrine Inhibits PD-L1 by Downregulating IFN-γ to Promote Ferroptosis and Enhance Anti-PD-L1 Efficacy in Liver Cancer

Yixi Nong[1–4,*], Houji Qin[2,3,*], Liyan Wei[2,5], Xi Wei[2,5], Jiannan Lv[2,3], Xiaoyi Huang[6], Biaoliang Wu[1,2,4,7]

[1]The First Clinical Medical College of Jinan University, Guangzhou, 510000, People's Republic of China; [2]Affiliated Hospital of Youjiang Medical University for Nationalities, Baise, Guangxi, 533000, People's Republic of China; [3]Department of Infectious Diseases, Affiliated Hospital of Youjiang Medical University for Nationalities, Baise, Guangxi, 533000, People's Republic of China; [4]National Immunological Laboratory of Traditional Chinese Medicine, Baise, Guangxi, 533000, People's Republic of China; [5]Health Management Center, Affiliated Hospital of Youjiang Medical University for Nationalities, Baise, Guangxi, 533000, People's Republic of China; [6]Youjiang Medical University for Nationalities, Baise, Guangxi, 533000, People's Republic of China; [7]Department of Endocrinology, Affiliated Hospital of Youjiang Medical University for Nationalities, Baise, Guangxi, 533000, People's Republic of China

*These authors contributed equally to this work

Correspondence: Biaoliang Wu, Department of Endocrinology, Affiliated Hospital of Youjiang Medical University for Nationalities, 18 Zhongshan second Road, Baise, Guangxi, 533000, People's Republic of China, Email yymucun@ymun.edu.cn

Purpose: Oxymatrine has potent anti-cancer activity, but its exact mechanism in liver cancer remains elusive. The present study was designated to explore oxymatrine's effect and the potential mechanism on Programmed cell death-ligand 1 (PD-L1) expression and ferroptosis in liver cancer.

Methods: Oxymatrine's influence on PD-L1 expression and ferroptosis-related proteins in liver cancer cells was explored in vitro and in vivo utilizing Western blotting, qRT-PCR, immunofluorescence, ELISA, H&E staining, immunohistochemistry, as well as detection of Fe^{2+}, ROS, and MDA.

Results: The in-vivo results showed that xenotransplanted tumor mice with drug interventions (oxymatrine, anti-PD-L1, and combination groups) exhibited inhibited tumor growth compared to control mice. Relative to anti-PD-L1 administration alone, the combined treatment inhibited tumor growth more significantly, along with reduced interferon-γ (IFN-γ) expression in peripheral blood and remarkably increased tumor immune lymphocyte ($CD4^+$ T and $CD8^+$ T) infiltration in cancer tissues. Meanwhile, PD-L1, xCT, and GPX4 protein levels in the combination group were significantly downregulated. According to the in vitro results, IFN-γ promoted PD-L1, xCT, and GPX4 protein levels in liver cancer cell lines. Oxymatrine reversed IFN-γ-induced upregulation of PD-L1 expression; moreover, it downregulated xCT and GPX4 protein levels in liver cancer cells and promoted intracellular Fe^{2+}, ROS, and MDA levels.

Conclusion: Oxymatrine promotes tumor immune response and ferroptosis in liver cancer by downregulating IFN-γ and synergistically enhances the inhibitory effect of anti-PD-L1 on liver cancer.

Keywords: oxymatrine, PD-L1, interferon-γ, ferroptosis, anti-PD-L1

Introduction

Immunotherapy holds significant promise in clinical applications for treating patients with advanced liver cancer. Immune checkpoint inhibitors (ICIs), such as anti-PD-L1 and anti-PD-1 antibodies, can enhance anti-tumor immunity, which restores the killing effect of tumor immune lymphocytes on tumors by blocking PD-L1 binding with PD-1, inhibit tumor immune escape, thus achieving the anti-tumor effect. Although ICI therapy has demonstrated encouraging outcomes in most tumors,[1,2] only 20–40% of patients can benefit from it due to low response rate and drug resistance.[3] Hence, investigating the mechanism of improving the therapeutic effect of ICIs is urgently needed.

Received: 13 September 2024
Accepted: 28 November 2024
Published: 6 December 2024

To sustain survival, tumor cells undergo metabolic reprogramming and alter the immunosuppressive microenvironment. It's resistance of ICIs is associated with abnormal upregulation of PD-L1.[4] The abnormally upregulated PD-L1 contributes to immune escape by restraining cytotoxic T lymphocytes' killing effects on tumors. PD-L1 regulation involves various mechanisms, among which IFN-γ induction has been shown as a major PD-L1 source in many tumors.[5] IFN-γ can induce PD-L1 expression in diverse tumor cells, which can bind with PD-1 to trigger CD8+ T cell senescence and apoptosis, reduce tumor immune cell infiltration, cause adaptive resistance of tumors, and eventually result in immunotherapy insensitivity.[6,7] This may be the reason for the unsatisfactory results of PD-1/PD-L1 therapy. Therefore, developing drugs that can reduce IFN-γ-induced PD-L1 expression is of great significance in improving the sensitivity of liver cancer immunotherapy.

Oxymatrine is an alkaloid in the roots of the Sophora genus plants, which has been proven to suppress tumor occurrence and development by promoting tumor cell apoptosis while repressing tumor cell proliferation, invasion, and migration; moreover, it is crucial in oxidative stress, immune regulation, and other disease links.[8–10] Oxymatrine can enhance anti-PD-L1's therapeutic role against lung adenocarcinoma in a mouse model.[11] Moreover, oxymatrine can also reverse IFN-γ-caused PD-L1 upregulation in human colorectal cancerous cells and melanoma cells[12,13] suggesting that oxymatrine may elevate ICIs' anti-tumor effect by regulating IFN-γ-triggered PD-L1 expression and is expected to become a drug to assist tumor immunotherapy.

Ferroptosis is an iron-driven cell death modality characterized by intracellular lipid peroxides accumulation, mitochondrial reactive oxygen species (ROS) generation, the decline of cystine/glutamate antiporter xCT, and the massive depletion of glutathione peroxidase 4 (GPX4).[14,15] IFN-γ suppresses ferroptosis by enhancing GPX4 expression in liver cancer stem cells,[16] which indicates that IFN-γ not only upregulates PD-L1 to facilitate immune escape but also expedites tumor development by inhibiting ferroptosis. Compelling evidence has confirmed that the combined regulation of PD-L1 and ferroptosis can synergistically enhance the anti-tumor effect.[17,18] In addition, downregulated PD-L1 expression augments CD8+ T cell viability, increases cancer cell ferroptosis, and improves anti-PD-1's therapeutic effect.[19] Targeted induction of ferroptosis could enhance the anticancer effect of anti-PD-1 in liver cancer,[20] implying the crucial functionality of ferroptosis in tumor immunity. Therefore, loosening IFN-γ's regulation in PD-L1 and ferroptosis may improve the efficacy of anti-tumor immunotherapy. However, whether oxymatrine can mediate ferroptosis has not been determined. Based on the above research findings, it is reasonable to speculate that oxymatrine may regulate ferroptosis by interfering with IFN-γ's regulation in PD-L1.

Currently, little is known about the regulatory mechanism of oxymatrine on PD-L1 and ferroptosis. Therefore, exploring the effect and underlying mechanism of oxymatrine on PD-L1 and ferroptosis in liver cancer is greatly important. This study observes the effects of oxymatrine and its combination with ICIs on tumor growth in xenotransplanted mice and further explores the effect of oxymatrine interfered IFN-γ on PD-L1 and ferroptosis in liver cancer cells in vitro. This study may offer a reference for studying the mechanism of improving the effect of liver cancer immunotherapy.

Materials and Methods

Reagents Preparation

IFN-γ was supplied by PeproTech (300–02); oxymatrine (purity 99.52%) was procured from RHAWN (R096543); InVivoMAb anti-mouse PD-L1 was supplied by BioXcell (BE0101). Rabbit PD-L1 Antibody was obtained from Gene Tex (GTX635973); Rabbit Anti-PD-L1 antibody was from Bioss (bs-22022R); CD4 Polyclonal Antibody was purchased from UpingBio (YP-Ab-13902); the following antibodies were provided by Affinity: xCT Antibody (DF12509), GPX4 Antibody (DF6701), GAPDH Antibody (AF7021), CD8 Antibody (AF5126).

Cell Culture

Human (HEPG2, MHCC97H) and mouse (H22) liver cancer cell lines (Pricella, Wuhan, China) were incubated (5% CO_2, 37°C in high-glucose DMEM and RPMI-1640 medium, respectively, containing 10% fetal bovine serum (FBS) (Pricella, 164210–50) and 1% penicillin-streptomycin (Solarbio, SV30010). During the treatment process, cells receiving

IFN-γ exposure were induced (24 h) by IFN-γ (0, 5, 10, 20, and 40ng/mL).[21] Then, cells received treatment with IFN-γ and oxymatrine (1, 2, and 4mg/mL) for 24 h.[13,22,23]

Mouse Xenograft Experiments

All animal experimental procedures followed the animal protocols and got approval from the Ethics Committee for Laboratory Animal Management of Youjiang Medical University For Nationalities. Immunocompetent BALB/c male mice (4–6 weeks; Vital River Laboratory Animal Technology Co., Ltd., Guangdong, China) were raised in specific pathogen-free (SPF) conditions and grouped into the normal (n = 4) and model group (n = 16) at random. For the model group of mice, H22 cell suspension (5×10^7 cells/mL) preparation was conducted using 1 × phosphate buffer saline (PBS) (Solarbio, P1020). Next, a mouse xenograft model of liver cancer was established through subcutaneous injection of 200 μL of cell suspension in the mouse right axilla. The xenograft tumor length reaching 0.5 cm indicated that the model was successfully established. Further, mice in the model group were sub-grouped (n = 4) at random: control, oxymatrine, anti-PD-L1, and oxymatrine + anti-PD-L1 groups (combination). Mice in the treatment group were injected intraperitoneally every other day with 100 mg/mL of oxymatrine and 200 μg of anti-PD-L1, twice a week and 7 injections in total, 200 μL each time. The control mice were intraperitoneally injected with an equal amount of 200 μL 1 × PBS. A vernier caliper: $V = 1/2 \times (\text{length} \times \text{width}^2)$ was utilized to measure xenograft tumor volume (V) every 4 days. One day after the end of administration, mouse peripheral blood samples were collected. After mouse euthanasia through cervical dislocation, tumors were dissected, weighed, and removed. Afterward, 10% of the tumor bodies were soaked in 4% paraformaldehyde (Solarbio, P1110) for staining with hematoxylin and eosin and immunohistochemistry, while other tumor tissues were employed for the subsequent testing. The dosage of oxymatrine[24,25] and anti-PD-L1[11] were referenced from previous studies, respectively.

Detection of IFN-γ by Enzyme-Linked Immunosorbent Assay

IFN-γ level in mouse peripheral blood supernatant was detected following the mouse IFN-γ ELISA Kit's instructions (RUIXIN BIOTECH, RX203097M). The final concentration of IFN-γ was calculated by equation after determination of the optical density (OD) value using a multifunctional microplate reader (PerkinElmer; Shanghai, China).

H&E Staining

After 24-h fixing in 4% paraformaldehyde fixative, the dissected 10% xenograft tumor tissues were dehydrated, paraffin-embedded, and cut into slices (4 μm). Next, following dewaxing in an oven at 70°C for 90 min, the tissue sections were washed and hydrated in xylene, and then washed with distilled water after gradient ethanol precipitation (100%, 95%, 85%, and 75%). Subsequently, after hematoxylin (Beyotime, ST2067) staining, the sections underwent differentiation in 1% hydrochloric acid alcohol, and then eosin (Beyotime, C0109) staining. Finally, the sample sections were immersed in gradient ethanol and xylene, followed by neutral resin sealing (Solarbio, G8590). A microscope (400 × magnification) was employed for observation.

Immunohistochemistry

The sectioned tissues were dewaxed, hydrated, and boiled with sodium citrate under high pressure for 10 min for antigen retrieval. The operations were conducted following the manufacturer's protocols of the Two-step Immunohistochemistry Kit (Elabscience, E-IR-R217). Briefly, after treating (10 min) with 3% catalase and blocking (normal goat serum), the sections were incubated (2 h, room temperature) with anti-CD8 and anti-CD4 antibodies. Next, the secondary antibody was added for incubation (30 min, room temperature), followed by PBS rinsing. Following DAB staining, the sections were counterstained and dehydrated. After the final neutral resin sealing, a microscope was utilized for cell staining observation. Three visual fields were captured at 400 × magnification using Image J software to calculate the positive cell numbers, and the average value was taken.

Immunofluorescence Assay

HEPG2 cells were placed onto 6-well plates for culturing. Cells then underwent 24h treatment with IFN-γ (10 ng/mL) of different concentrations with or without oxymatrine (4mg/mL), followed by 15-min fixing with 4% paraformaldehyde.

After reacting (30 min) with 1% bovine serum albumin (BSA), cells were incubated (4°C, overnight) with the primary antibody, followed by PBST washing and then 1h incubation with the secondary antibody (Abcam, ab150079) away from light. DAPI (Beyotime, P0131) was utilized for nuclei counterstain (10 min). An upright fluorescence microscope (Nikon; Japan) was employed for observation and photographing. The relative expression of the target protein was determined by fluorescence intensity analysis was utilized to determine using ImageJ software 3.0.

Fe^{2+} Detection

HEPG2 cells were cultured in fluorescent petri dish and treated (24 h) with IFN-γ (10 ng/mL) with or without oxymatrine (4mg/mL), followed by detecting Fe^{2+} level following the FerroOrange Assay Kit's instructions (DOJINDO, F374). Shortly, cells underwent incubation (37°C, CO_2, 30 min) with 1 mol/L FerroOrange working solution in the dark. A laser confocal microscope (Leica; Germany) was employed for cell signal observation and photographing. The fluorescence intensity determination was conducted utilizing ImageJ software 3.0.

Detection of Intracellular ROS

HEPG2 cells were placed onto 6-well plates, followed by 24-h IFN-γ (10 ng/mL) treatment with or without oxymatrine (4mg/mL) and then detection of ROS level as per the ROS Detection Kit's protocol (Beyotime, S0033M). After PBS washing, the cells were cultured (20 min) in 10 μ1 DCFH-DA-contained serum-free medium away from light and immediately observed under an upright fluorescence microscope (Nikon). The ImageJ software 3.0 was employed for fluorescence intensity determination.

Malondialdehyde Detection (MDA)

HEPG2 cells were cultured and treated with IFN-γ (10 ng/mL) with or without oxymatrine (4mg/mL) for 24 h. Then, after cell (1×10^7) collection, intracellular MDA content was measured utilizing a corresponding kit (DOJINDO, M496). A fluorescence microplate reader was employed for MDA fluorescence intensity detection. A standard curve of MDA was plotted to calculate the MDA actual concentration within the sample.

Quantitative Real-Time PCR

HEPG2 cell total RNA extraction was performed utilizing TRIzol^{TM} reagent (Thermo/Invitroge, 15596026). After purity and concentration determination, MonScript^{TM} RTIII Super Mix with dsDNase (Monad, MR05101M) was applied for single-stranded cDNA synthesis. qRT-PCR was conducted utilizing the MonAmp^{TM}SYBR Green qPCR Mix Kit (Monad, MQ10301S) to detect the mRNA level of relative gene. Data were collected using the LightCycler96 system (Roche; Germany). The $2^{-\Delta\Delta Ct}$ method was utilized for data calculation. Glyceraldehyde-3-phosphate dehydrogenase (GAPDH) served as an internal control. The primer sequences used in PCR reaction were as follows: CD274 was synthesized by Gene Create (Wuhan, China): CD274-F: GGAGATTAGATCCTGAGGAAAACCA;CD274-R:AACGGAAGATGAATGTC AGTGCTA; GAPDH was synthesized by Genesys (USA): GAPDH-F: CAGGAGGCATTGCTGATGAT; GAPDH-R: GAAGGCTGGGGCTCATTT.

Western Blotting

Cells and animal tissues were collected, and the radio-immunoprecipitation assay (RIPA) lysis buffer (Solarbio, R0020) supplemented with protease inhibitor (phenylmethylsulfonyl fluoride) (Solarbio; P1260) was employed for cell lysis. The protein gray value (OD value) was measured using a bicinchoninic acid (BCA) kit (Beyotime, P0010S). Protein concentration was calculated by plotting a protein standard curve. After lysis, 5 × sodium dodecyl-sulfate polyacrylamide gel electrophoresis (SDS-PAGE) protein loading buffer (Solarbio, PG11X) was mixed with cells, followed by 10 min boiling (100°C). Cells were subjected to 10% SDS-PAGE for protein separation, which was then transferred to the polyvinylidene fluoride (PVDF) membranes. After 30-min blocking (room temperature) in protein-free rapid blocking solution (Solarbio, PS108), the membranes underwent incubation (4°C with the primary antibody, followed by a further 1 h incubation (room temperature) with the secondary antibody (Invitroge, C31460100). A chemiluminescence imaging system (UVItec; UK)

and chemiluminescence reagent (Epizyme, SQ201) were applied for target protein band observation. Target protein bands' grayscale values were measured utilizing the ImageJ software 3.0.

Statistical Analysis

All data are shown in the form of mean ± standard deviation. Statistical analysis and visualization were conducted utilizing GraphPad Prism 9.0. The difference between the two groups was compared by adopting the *t*-test, and that among multiple groups was compared utilizing the one-way or two-way analysis of variance (ANOVA). $P < 0.05$ represented a difference with statistical significance.

Results

Oxymatrine Combined with Anti-PD-L1 Inhibits Tumor Growth in vivo and Synergistically Enhances Anti-PD-L1's Anti-Tumor Effect

We established a xenograft model of liver cancer in mice. It was observed that tumor size and volume and tumor growth curve in the oxymatrine, anti-PD-L1, and combination groups were decreased relative to those in the control group, indicating that both oxymatrine and anti-PD-L1 interventions inhibited tumor growth, and the inhibition of tumor growth was more significant in the combination group than that in the anti-PD-L1 group ($P < 0.0001$) (Figure 1A–C). And, Mouse body weight exhibited no significant difference in each group (Figure 1D). As shown by H&E staining results, mice with drug interventions (oxymatrine, anti-PD-L1, and combination groups) exhibited histological disorder and enhanced inflammatory infiltration and cell apoptosis relative to the control mice. Moreover, the combination group was more pronounced than the single drug groups, as shown in Figure 1E. Next, IFN-γ expression in mouse peripheral blood was detected using ELISA (Figure 1F). IFN-γ expression was elevated in the model group relative to that in the normal group, which, however, was decreased by oxymatrine, anti-PD-L1, and combination treatments, with the combination group showing the most significant decrease in IFN-γ expression. $CD8^+$ and $CD4^+$ T lymphocyte infiltration were detected using immunohistochemistry (Figure 1G–I) for further exploring the effect of oxymatrine combined with anti-PD-L1 in tumor immune cells. According to the results, promoted $CD8^+$ T cell infiltration in tumor tissues in the oxymatrine and anti-PD-L1 groups was observed relative to that in the control group, which was more significant in the combination group than the anti-PD-L1 group. As for $CD4^+$ T cell infiltration, elevated $CD4^+$ T cell infiltration in tumor tissues in the anti-PD-L1 group was observed compared with the control group; additionally, notably increased $CD4^+$ T cell numbers in the combination group were also found relative to the anti-PD-L1 group.

In addition, we performed Western blotting to detect PD-L1, xCT, and GPX4 levels in various tumor tissues to investigate the relevant mechanisms underlying oxymatrine's role in vivo. As shown in Figure 1J and K, the oxymatrine, PD-L1, and combination groups showed downregulated PD-L1 and GPX4 protein levels ($P < 0.01$); additionally, the combination group exhibited a more significant downregulation of these proteins was more significant than the anti-PD-L1 group.

IFN-γ Upregulates PD-L1 Protein Level in Liver Cancer Cells

Thereafter, we using Western blotting to investigate the regulatory role of IFN-γ in PD-L1 in liver cancer cells. It was found that PD-L1 level in HEPG2 cells was upregulated after IFN-γ intervention, especially at the concentration of 10–20 ng/mL, with significant differences ($P < 0.05$) (Figure 2A) and no dose dependence. Next, We obtained the similar results in MHCC97H and H22 cells (Figure 2B and C).

IFN-γ Promotes the Expressions of Ferroptosis-Related Proteins in Liver Cancer Cells

According to the results, IFN-γ intervention remarkably upregulated xCT and GPX4 protein levels in HEPG2, MHCC97H, and H22 cells, especially at concentrations of 10 and 20 ng/mL ($P < 0.05$) and no dose dependence (Figure 3A–C), indicating that IFN-γ upregulated ferroptosis-related protein levels in liver cancer cells.

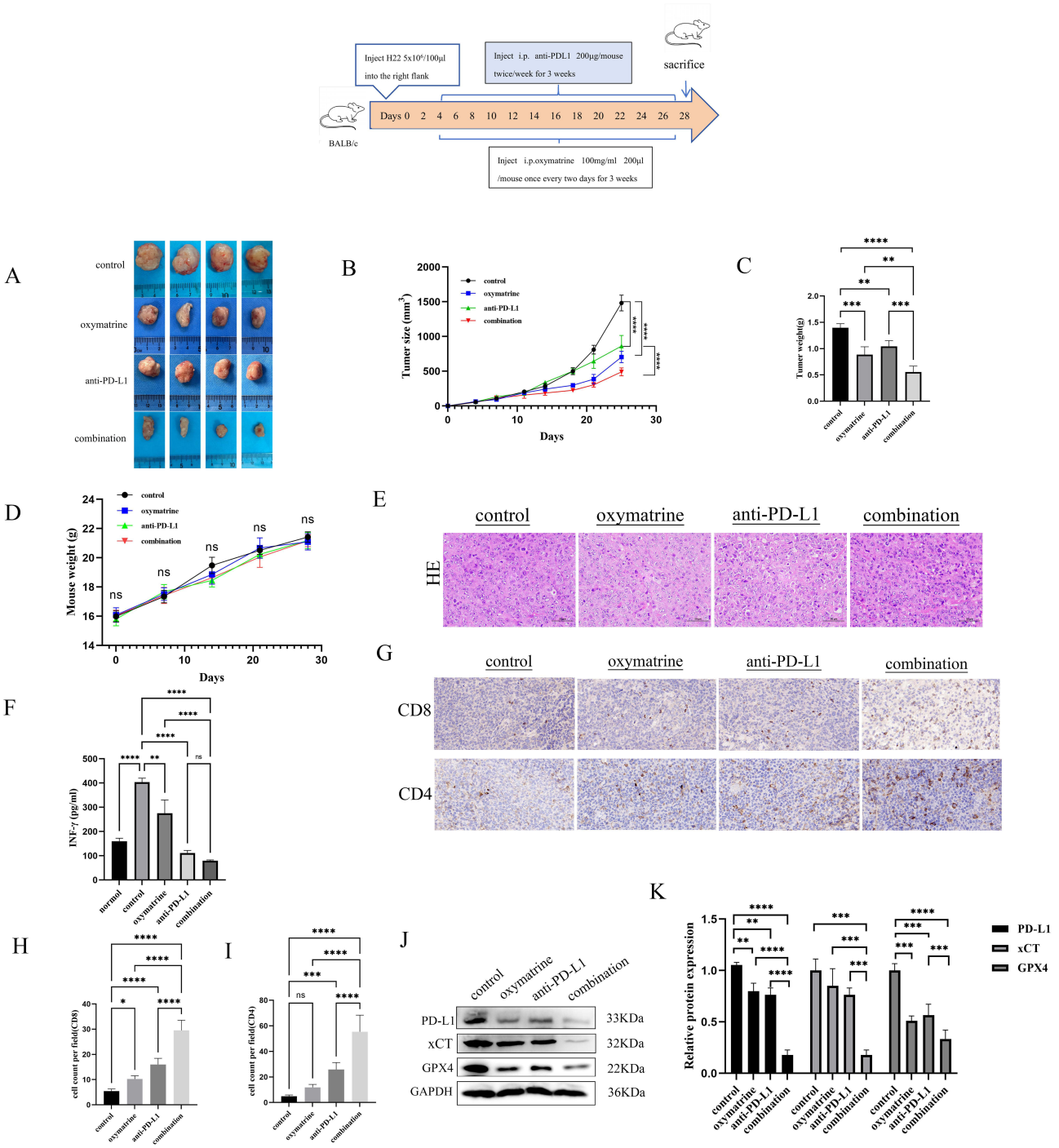

Figure 1 The inhibitory effect of oxymatrine on liver cancer-bearing mice. Mice in the treatment group were injected with 100 mg/mL of oxymatrine and 200 μg of anti-PD-L1. (**A**) Representative images of HCC xenografts. Xenograft tumors were measured (n=4). (**B**) Tumor growth curve (n=4). (**C**) Tumor weight (n=4). (**D**) Changes in mouse body weight (n=4). (**E**) Representative images of tumor tissues stained with H&E (n=4). Scale bar, 100 μm. (**F**) ELISA detection of IFN-γ expression in mouse peripheral blood of the normal and xenograft model groups (n=4). (**G**) Immunohistochemical detection of $CD8^+$ T and $CD4^+$ T cell infiltration in tumor tissues (n=4). (**H** and **I**) Quantitative bar charts of the relative expressions of positive $CD8^+$ T and $CD4^+$ T cells in tumor tissues (n=4). (**J**) Western blotting detection (n=4) and (**K**) Bar charts of PD-L1, xCT, and GPX4 protein levels in xenografts (n=4). ns, no statistical difference; *$P < 0.05$; **$P < 0.01$; ***$P < 0.001$; ****$P < 0.0001$.

Oxymatrine Reverses IFN-γ-Induced Upregulation of PD-L1 and Ferroptosis Related Proteins

To further investigate whether oxymatrine interfered with the expressions of PD-L1 and ferroptosis-related proteins xCT and GPX4 regulated by IFN-γ, we intervened liver cancer cells with oxymatrine (1, 2, and 4 mg/mL) and IFN-γ (10 ng/

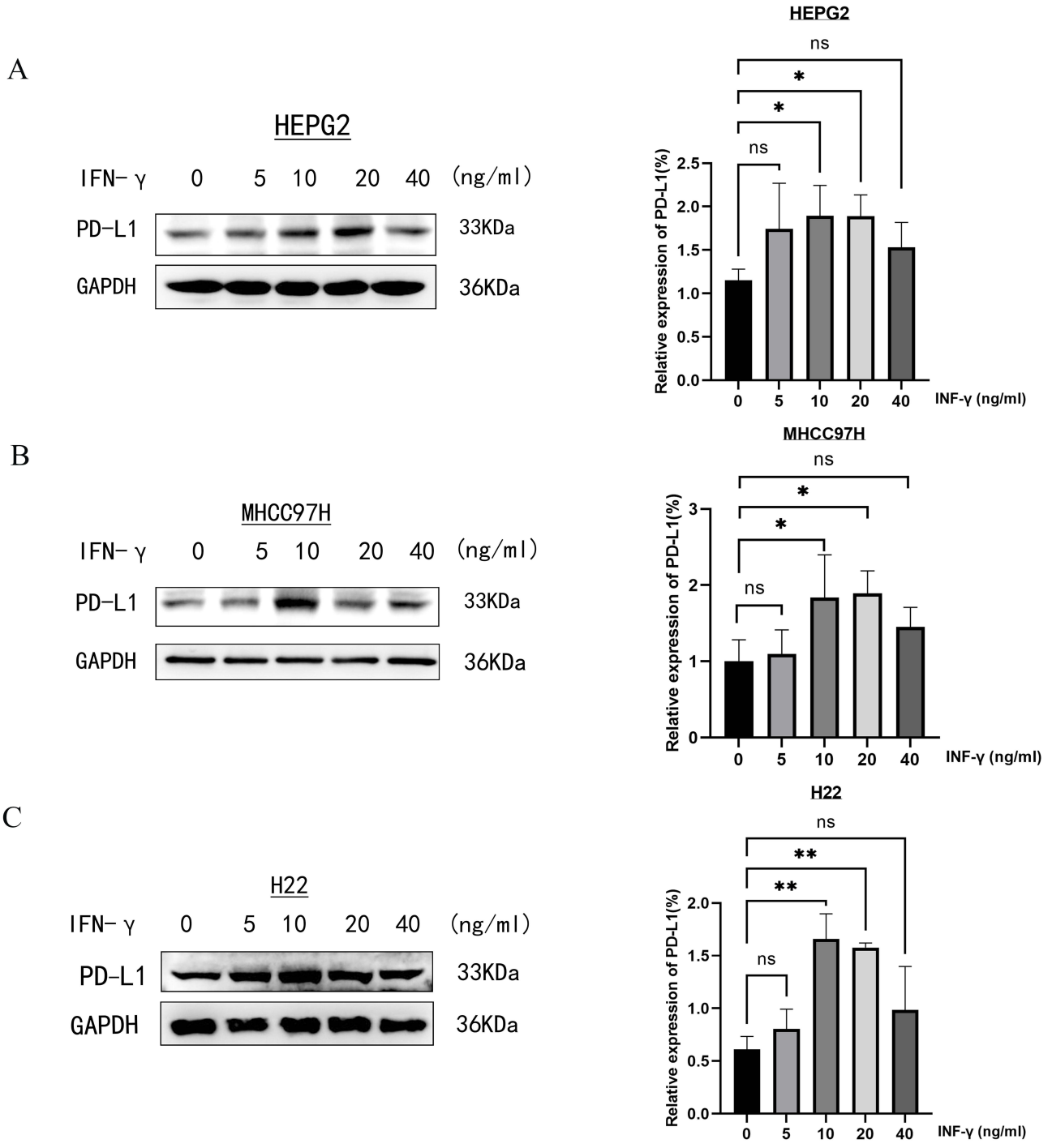

Figure 2 IFN-γ's effect on the expressions of PD-L1 protein in liver cancer cell lines. (**A-C**) Western blotting detection of PD-L1 protein level in HEPG2, MHCC97H, and H22 cells after 24-h intervention with IFN-γ (0, 5, 10, 20, and 40 ng/mL) (left), and bar charts of PD-L1 relative expression (right) (n=3). ns, no statistical difference; *$P < 0.05$; **$P < 0.01$.

mL and 20 ng/mL) and then detected PD-L1, xCT, and GPX4 protein levels. As shown in Figure 4A–C, oxymatrine exerted no significant impact on PD-L1, xCT, and GPX4 protein levels in HEPG2, MHCC97H, and H22 cells without IFN-γ exposure. However, oxymatrine reversed IFN-γ exposure-caused elevation of PD-L1, xCT, and GPX4 levels in liver cancer cells. Especially, an oxymatrine concentration of 4 mg/mL showing the most significant inhibitory effect at an IFN-γ concentration of 10 ng/mL ($P < 0.05$).

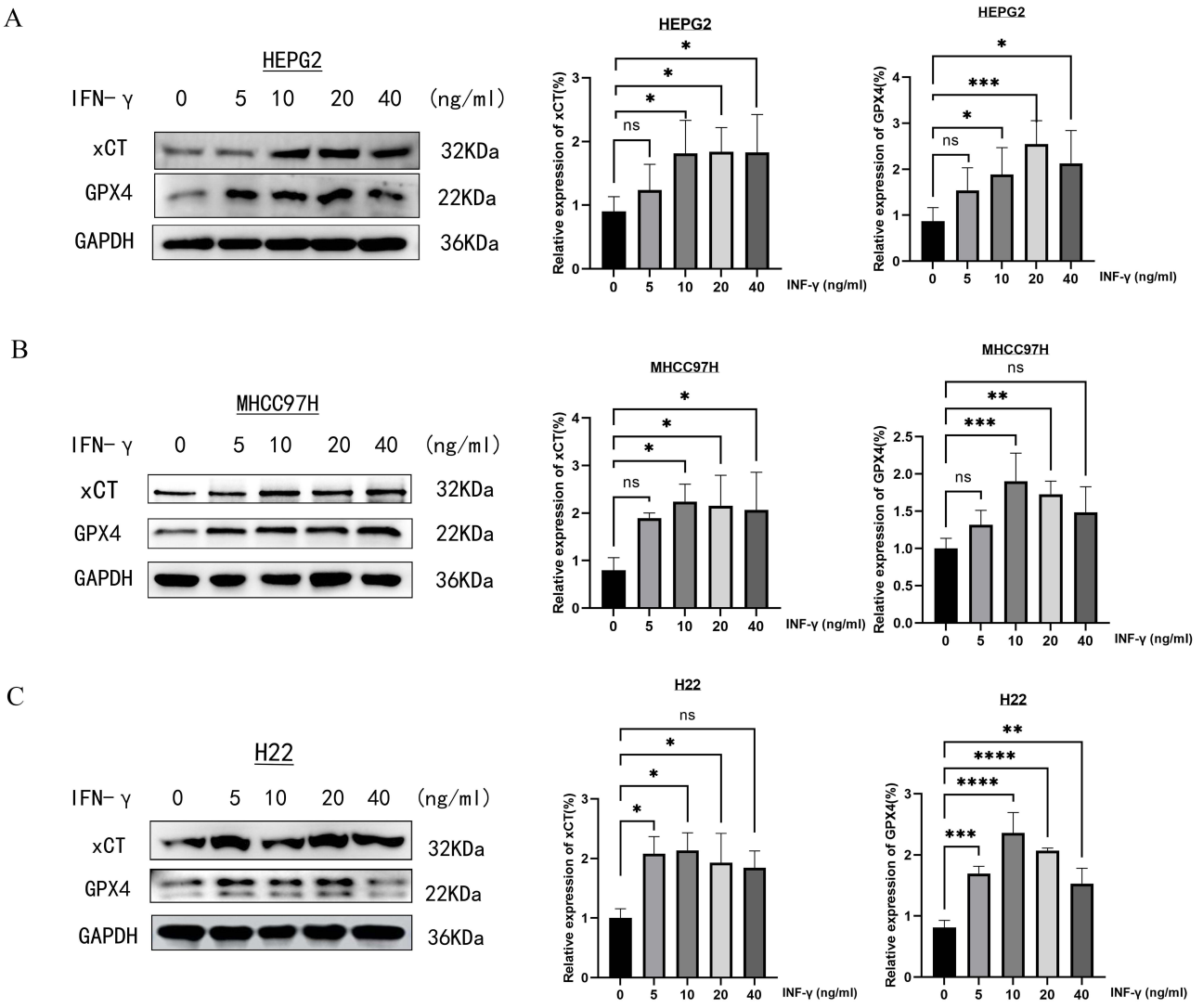

Figure 3 IFN-γ's effect on the expressions of ferroptosis-related proteins in liver cancer cell lines. (**A-C**) Western blotting detection of xCT and GPX4 protein levels in HEPG2, MHCC97H, and H22 cells after 24 h of intervention with IFN-γ (0, 5, 10, 20, and 40 ng/mL) (left), and bar charts of the relative expressions of xCT and GPX4 proteins (right) (n=3). ns, no statistical difference; **P* < 0.05; ***P* < 0.01; ****P* < 0.001; *****P* < 0.0001.

Based on the above research results, we have chosen the HepG2 cell line for subsequent studies. And the subsequent cell experiments were conducted using 10 ng/mL IFN-γ and 4 mg/mL oxymatrine. The immunofluorescence assay further confirmed that oxymatrine reversed IFN-γ's impact on PD-L1 protein level in HEPG2 cells. As shown in Figure 4D and E, the IFN-γ group showed an enhanced red fluorescence signal of HEPG2 cells relative to the control group; however, oxymatrine could weaken this red fluorescence signal, consistent with the results of Western blotting. The PD-L1 protein encodes the CD274 gene. CD274 mRNA expression in HEPG2 cells was detected using qRT-PCR. As shown in Figure 4F, the IFN-γ group showed a remarkably higher CD274 mRNA expression in HEPG2 cells than the control group, whereas oxymatrine could effectively decrease CD274 mRNA expression.

Oxymatrine Reverses the Inhibitory Effects of IFN-γ on Fe^{2+}, ROS, and MDA in HEPG2 Cells and Promotes Ferroptosis Occurrence

We continued to explore oxymatrine's effects on Fe^{2+}, ROS, and MDA in HEPG2 cells. We used the Fe^{2+} detection kit to measure the level of Fe^{2+} in cells and observed the strength of the red signal in cells under a microscope. According to the results, the red fluorescence signal was weakened in the IFN-γ group, but enhanced in the oxymatrine group relative

to the control group; oxymatrine could enhance the IFN-γ-weakened red fluorescence signal (Figure 5A and B). Next, ROS expression in HEPG2 cells was detected using the ROS detection kit. A microscope was used for green fluorescence signal observation. The IFN-γ group exhibited decreased, while the oxymatrine group showed increased green fluorescence signal relative to the control group; oxymatrine could enhance the IFN-γ decrease in green fluorescence signal (Figure 5C and D). Similarly, the intracellular MDA content was detected using the MDA assay kit. The OD values were obtained to calculate the concentration of MDA. As shown in Figure 5E, the intracellular MDA content was decreased in the IFN-γ group relative to the control group, but elevated in the oxymatrine group; the intracellular MDA content was relatively elevated in the IFN-γ + oxymatrine group.

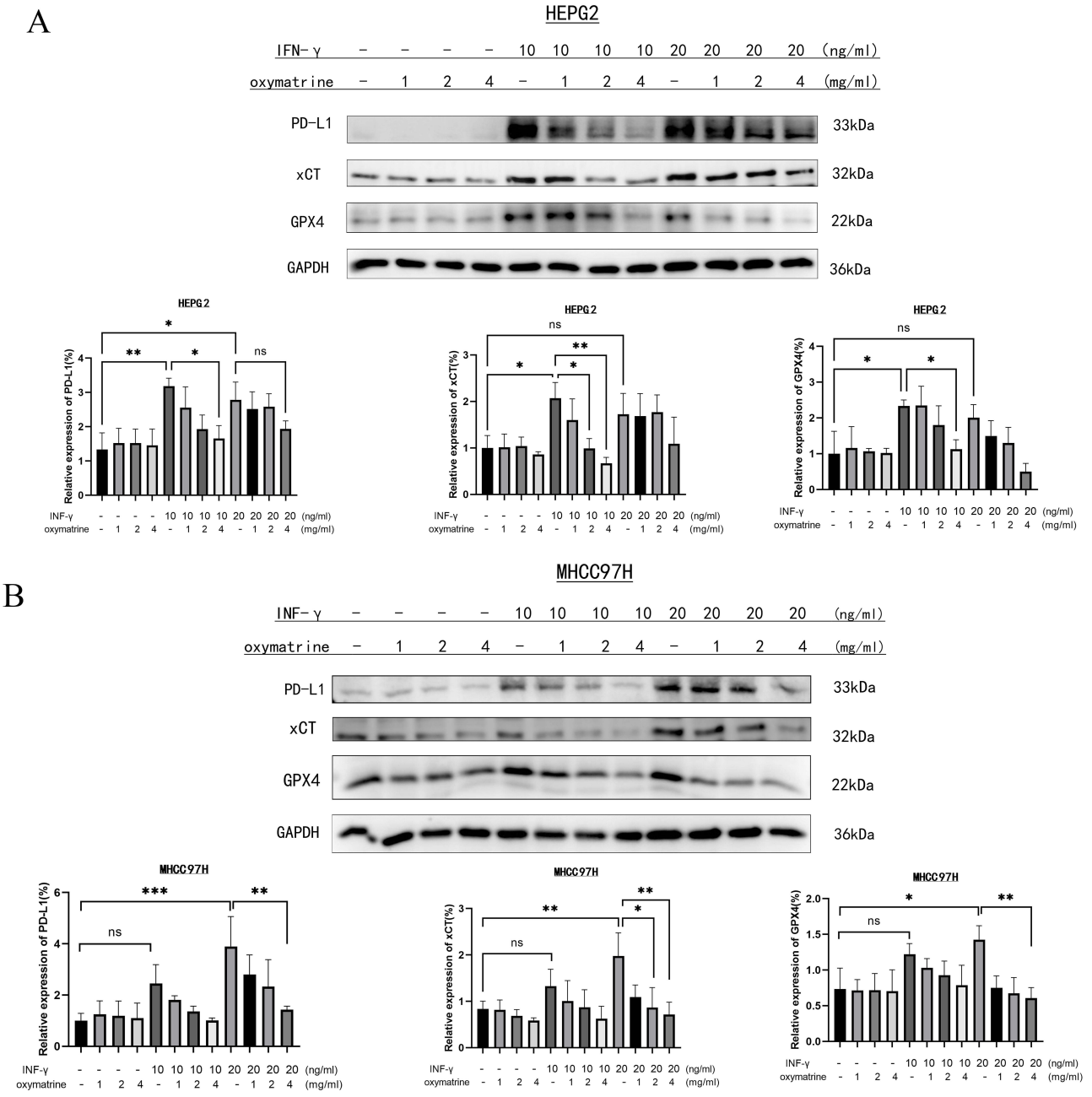

Figure 4 Continued.

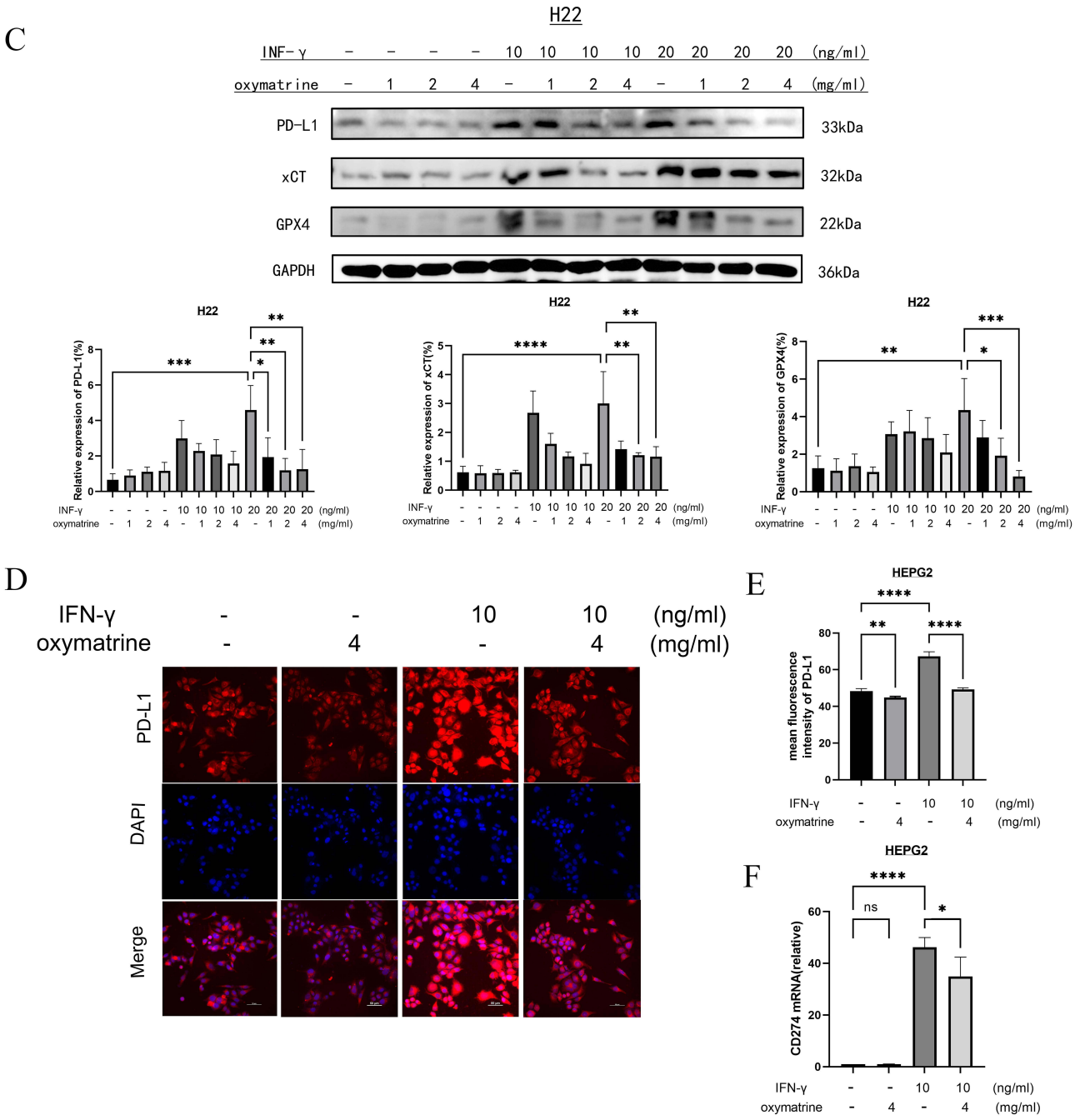

Figure 4 Oxymatrine intervenes in IFN-γ's role in PD-L1 and ferroptosis-related protein levels in liver cancer cell lines. (**A-C**) Western blotting detection of PD-L1, xCT, and GPX4 protein levels in HEPG2, MHCC97H, and H22 cells after 24 h of intervention with oxymatrine (0,1, 2, and 4 mg/mL) in exposure to IFN-γ (10, 20 ng/mL) (upper), and bar charts of the relative expressions of PD-L1, xCT and GPX4 proteins (lower) (n=3). (**D**) Immunofluorescence assay detection of PD-L1 protein in HEPG2 cells after 24 h of intervention with oxymatrine (4 mg/mL) in exposure to IFN-γ (10 ng/mL); a fluorescence microscope was used for cell observation, with red indicating PD-L1 protein-positive expression and blue indicating DAPI-stained nucleus (n=3); scale bar, 50 μm (left). (**E**) Fluorescence intensity histogram of PD-L1 protein relative expression in HEPG2 cells (right) (n=3). (**F**) RT-qRCR detection of CD274 mRNA relative expression in HEPG2 cells after 24 h of intervention with oxymatrine (4 mg/mL) in exposure to IFN-γ (10 ng/mL) (n=3). ns, no statistical difference; **P* < 0.05; ***P* < 0.01; ****P* < 0.001; *****P* < 0.0001.

Discussion

The application of ICIs has markedly enhanced cancer treatment in the last decade. However, only a few patients with advanced liver cancer respond. To evade immune attacks, tumors upregulate PD-L1 expression within the tumor microenvironment via IFN-γ, which can bind to PD-1 on the T lymphocyte surface, thus weakening T cells' killing

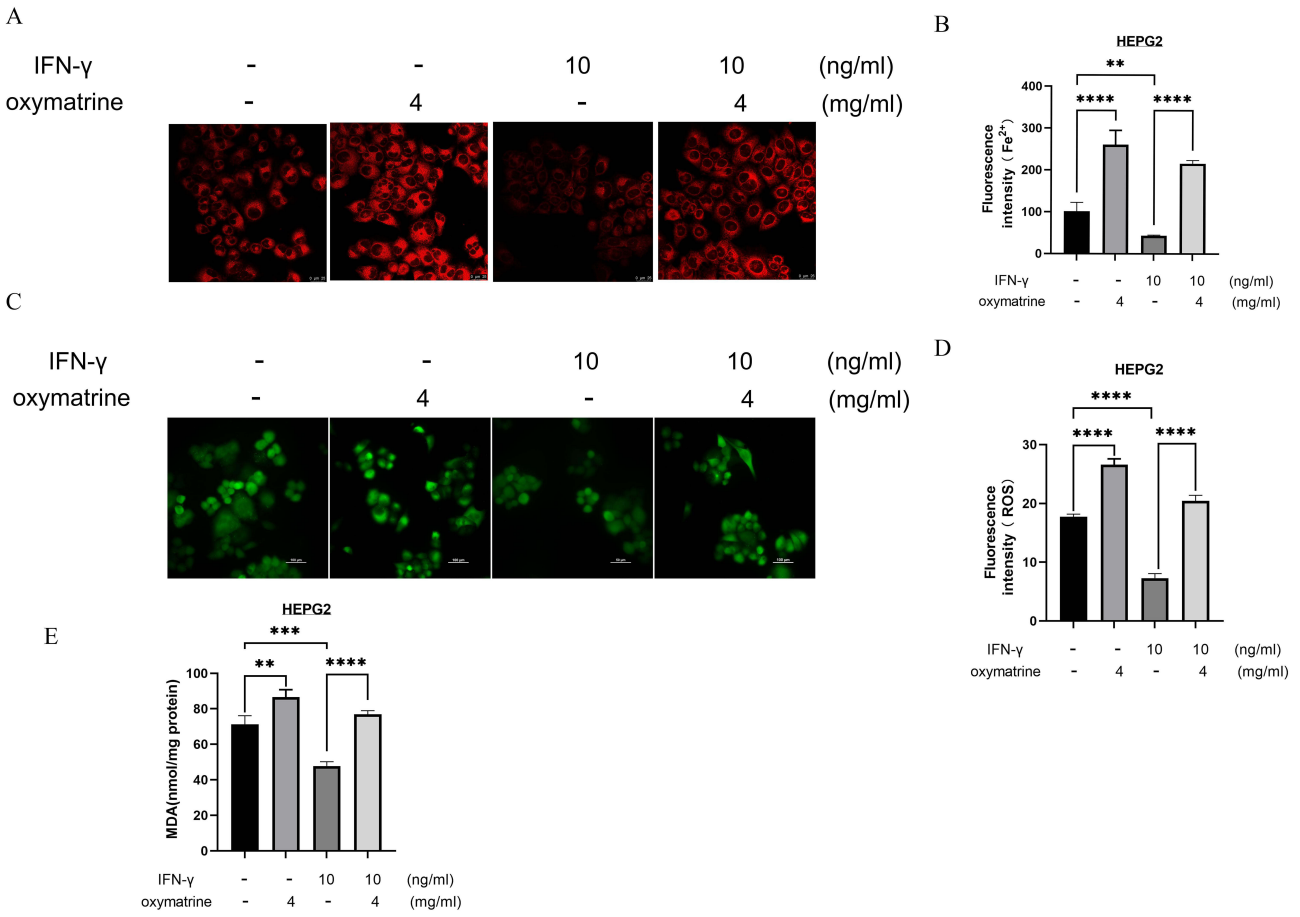

Figure 5 Oxymatrine intervenes in IFN-γ's role in ferroptosis in HEPG2 cells. HEPG2 cells underwent treatment with oxymatrine (4 mg/mL) with or without IFN-γ (10ng/mL) for 24 h. (**A**) Detection of Fe^{2+} expression using intracellular Fe^{2+} fluorescent probe (FerroOrange method); cells were observed under a laser confocal microscope (scale bar, 25 μm), with red light indicating Fe^{2+}-positive cells (n=3). (**B**) Quantitative plot of relative fluorescence intensity of intracellular Fe^{2+} expression (n=3). (**C**) Detection of intracellular ROS level using fluorescent probe DCFH-DA staining; cells were observed under a fluorescence microscope (scale bar, 50 μm), with green light indicating intracellular ROS-positive expression (n=3). (**D**) Quantitative bar chart of relative fluorescence intensity of intracellular ROS (n=3). (**E**) Detection of the intracellular MDA content using the MDA Assay Kit (n=3). $^{**}P < 0.01$; $^{***}P < 0.001$; $^{****}P < 0.0001$.

effects.[26] It is suggested that IFN-γ has an inhibitory effect on the established anti-tumor immune response of tumors, making them insensitive to ICI therapy. Therefore, effective treatment of liver cancer remains a major challenge.

Oxymatrine has been demonstrated to possess significant anti-tumor activity, but its mechanism of action on liver cancer is unclear yet. As observed in this study, oxymatrine suppressed liver cancer tissue growth and IFN-γ secretion in liver cancer-bearing mice. Oxymatrine combined with anti-PD-L1 could further slow tumor tissue growth and reduce IFN-γ secretion, indicating that oxymatrine inhibited liver cancer growth and enhanced anti-PD-L1's anticancer. In addition, combination therapy significantly downregulated PD-L1 protein level in tumor tissues, indicating that oxymatrine exerted anticancer effects by inhibiting IFN-γ expression in mouse peripheral blood and PD-L1 protein in tumor tissues. IFN-γ's effect on tumor microenvironment is quite complex. Under normal conditions, IFN-γ initially exhibits anti-tumor activity and increases antigen presentation. However, sustained IFN-γ can cause immune reprogramming in tumor cells already under tumor immune activation, and induce PD-L1 expression in tumor cells, thus facilitating tumor progression.[27] The abnormally upregulated PD-L1 within the tumor microenvironment is crucial for the resistance to anti-PD-1/PD-L1 therapy and an important cause of immune escape. Through in vitro simulation of IFN-γ exposure in liver cancer cells, IFN-γ intervention was found to upregulate PD-L1 expression in different liver cancer cells, and the results were consistent with expectations,[16,20] indicating that IFN-γ may participate in regulating PD-L1 in liver cancer. Further, oxymatrine downregulated PD-L1 expression in cells with IFN-γ exposure. The in vivo experiment results are consistent with those of in vitro experiments. Moreover, we found that oxymatrine inhibited IFN-γ-caused upregulation

of CD274 mRNA and regulated CD274 expression at the transcriptional level. The PD-L1 protein is encoded by the CD274 gene. IFN-γ elevates PDL1 expression through binding to the CD274 gene promoter.[28] Collectively, according to the in vitro and in vivo results, oxymatrine can inhibit PD-L1 expression by reducing IFN-γ.

The extensive research on ferroptosis has boosted a perspective for its application in cancer therapeutics. We found in vivo experiments that oxymatrine downregulated IFN-γ, PD-L1, xCT, and GPX4 expressions simultaneously, but the specific regulatory relationship remained unknown. Exposure to IFN-γ enhances GPX4 expression in liver cancer stem cells and inhibits ferroptosis occurrence.[16] In vitro, IFN-γ upregulated PD-L1 expression in liver cancer cells, while upregulating ferroptosis-related protein (xCT and GPX4) levels, indicating that IFN-γ could regulate ferroptosis-related proteins in liver cancer. We further observed that oxymatrine reversed the upregulation of xCT and GPX4 in liver cancer cells induced by IFN-γ exposure, while offsetting IFN-γ's inhibition on Fe^{2+}, lipid ROS, and MDA generation in HEPG2 cells, indicating that oxymatrine promoted ferroptosis by downregulating IFN-γ. However, a previous study has reported that knocking down the PD-L1 gene in liver cancer cells enhances the effect of ferroptosis.[16] PD-L1 is an upstream regulatory factor of GPX4. Moreover, Blocking PD-L1 expression in cancer cells helps to inhibit IFN-γ-mediated tumor-promoting effect.[27] Taken together, IFN-γ may inhibit ferroptosis occurrence via upregulating PD-L1 and GPX4 expressions. Therefore, oxymatrine downregulated IFN-γ and PD-L1, thereby suppressing the expressions of xCT and GPX4 and ultimately facilitating ferroptosis in liver cancer.

Additionally, tumor resistance to ICIs is tightly associated with the abnormal number and function of T cells. The blocking impact of PD-1/PD-L1 depends on T cell function.[4] CD4+ T cells can assist in promoting CD8+ T cells' killing effects on tumors. Patients with low response or resistance to ICI therapy often exhibit functional impairment or failure of CD4+ T and CD8+ T cells. GPX4 deficiency in the liver contributes to the increased CD8+ T cells within the immune microenvironment.[29] Subsequently, activated CD8+ T lymphocytes accelerate ferroptosis occurrence in tumors.[19,30] We found that oxymatrine combined with anti-PD-L1 significantly promoted CD8+ and CD4+ T lymphocyte infiltration in tumor tissues while downregulating ferroptosis proteins (xCT and GPX4), which indicated that the combination therapy enhanced liver cancer immune activity and ferroptosis occurrence. Mechanistically, the stronger the activity of T lymphocytes in the body, the more IFN-γ is released. Interestingly, on the contrary, we observed in vivo that oxymatrine increased tumor immune cell infiltration, while the level of IFN-γ in tumor-bearing mouse peripheral blood was decreased. This is potentially associated with the complex role of IFN-γ in tumors. Chenmin et al[31] found in the study of gastric cancer that the traditional Chinese medicine asiaticoside improved CD8+ T cell percentage and IFN-γ concentration in vitro while reducing GPX4, SLC7A11, PD-L1, and IFN-γ expressions in vivo, thereby promoting ferroptosis and inhibiting immune escape, which were consistent with our in vivo experimental results. Therefore, oxymatrine can promote tumor immune activity by downregulating IFN-γ, thereby promoting ferroptosis and ultimately contributing to anti-PD-L1's anticancer effect. However, there are still some limitations in this study. This study did not further explore the regulatory effect of oxymatrine on IFN-γ, nor did it set up a positive control group for a more comprehensive drug efficacy evaluation. Furthermore, this study did not further demonstrate the impact of oxymatrine on the regulatory relationship between liver cancer immune function and ferroptosis through bidirectional validation. We will further conduct and supplement relevant experiments in future.

All in all, the present study pioneers the idea that oxymatrine can suppress PD-L1 expression via downregulating IFN-γ, thereby restoring or promoting tumor immune cell activity, facilitating ferroptosis, and synergistically contributing to anti-PD-L1's inhibitory impact on liver cancer. Oxymatrine combined with anti-PD-L1 is a promising method of liver cancer immunotherapy with lower toxicity and higher effectiveness.

Informed Consent

For this type of study, no informed consent is required.

Ethics Approval

The study was approved by the Ethics Committee for Laboratory Animal Management of Youjiang Medical University For Nationalities (Approval No.:2023062101). The name of the guidelines followed for the welfare of the laboratory animals:GB/T 35892-2018 and Guide for the Care and Use of Laboratory Animals.

Acknowledgments

We would like to thank all the participants who participated in this study.

Author Contributions

All authors made a significant contribution to the work reported, whether that is in the conception, study design, execution, acquisition of data, analysis and interpretation, or in all these areas; took part in drafting, revising or critically reviewing the article; gave final approval of the version to be published; have agreed on the journal to which the article has been submitted; and agree to be accountable for all aspects of the work.

Funding

This work was supported by the key program of Guangxi Science Natural Foundation (No. 2023 GXNSFDA026008), the 2019 High-level Talent Research Project of the Affiliated Hospital of Youjiang Medical University for Nationalities (No.R20196333) and the Autonomous Region Traditional Chinese Medicine Bureau 2020 Self-Funded Scientific Research Project (No. GZZC2020255).

Disclosure

The authors declare that they have no conflict of interest.

References

1. Chen L, Han X. Anti-PD-1/PD-L1 therapy of human cancer: past, present, and future. *J Clin Invest*. 2015;125(9):3384–3391. doi:10.1172/jci80011
2. Constantinidou A, Alifieris C, Trafalis DT. Targeting programmed cell death −1 (PD-1) and ligand (PD-L1): a new era in cancer active immunotherapy. *Pharmacol Ther*. 2019;194:84–106. doi:10.1016/j.pharmthera.2018.09.008
3. Shimada Y, Matsubayashi J, Kudo Y, et al. Serum-derived exosomal PD-L1 expression to predict anti-PD-1 response and in patients with non-small cell lung cancer. *Sci Rep*. 2021;11(1):7830. doi:10.1038/s41598-021-87575-3
4. Sun JY, Zhang D, Wu S, et al. Resistance to PD-1/PD-L1 blockade cancer immunotherapy: mechanisms, predictive factors, and future perspectives. *Biomark Res*. 2020;8:35. doi:10.1186/s40364-020-00212-5
5. Garcia-Diaz A, Shin DS, Moreno BH, et al. Interferon receptor signaling pathways regulating PD-L1 and PD-L2 expression. *Cell Rep*. 2017;19(6):1189–1201. doi:10.1016/j.celrep.2017.04.031
6. Zhang X, Zeng Y, Qu Q, et al. PD-L1 induced by IFN-gamma from tumor-associated macrophages via the JAK/STAT3 and PI3K/AKT signaling pathways promoted progression of lung cancer. *Int J Clin Oncol*. 2017;22(6):1026–1033. doi:10.1007/s10147-017-1161-7
7. Fu Q, Liu X, Xia H, et al. Interferon-gamma induces immunosuppression in salivary adenoid cystic carcinoma by regulating programmed death ligand 1 secretion. *Int J Oral Sci*. 2022;14(1):47. doi:10.1038/s41368-022-00197-x
8. Li J, Liang J, Zeng M, et al. Oxymatrine ameliorates white matter injury by modulating gut microbiota after intracerebral hemorrhage in mice. *CNS Neurosci Ther*. 2023;29 Suppl 1(Suppl 1):18–30. doi:10.1111/cns.14066
9. Li Y, Yu P, Fu W, et al. Ginseng-Astragalus-oxymatrine injection ameliorates cyclophosphamide-induced immunosuppression in mice and enhances the immune activity of RAW264.7 cells. *J Ethnopharmacol*. 2021;279:114387. doi:10.1016/j.jep.2021.114387
10. Hu G, Cao C, Deng Z, et al. Effects of matrine in combination with cisplatin on liver cancer. *Oncol Lett*. 2021;21(1):66. doi:10.3892/ol.2020.12327
11. Zheng C, Xiao Y, Chen C, et al. Systems pharmacology: a combination strategy for improving efficacy of PD-1/PD-L1 blockade. *Brief Bioinform*. 2021;22(5). doi:10.1093/bib/bbab130
12. Hua S, Gu M, Wang Y, et al. Oxymatrine reduces expression of programmed death-ligand 1 by promoting DNA demethylation in colorectal cancer cells. *Clin Transl Oncol*. 2021;23(4):750–756. doi:10.1007/s12094-020-02464-x
13. Li X, He L, Ou Y, et al. Oxymatrine inhibits melanoma development by modulating the immune microenvironment and targeting the MYC/PD-L1 pathway. *Int Immunopharmacol*. 2023;124(Pt B):111000. doi:10.1016/j.intimp.2023.111000
14. Riegman M, Sagie L, Galed C, et al. Ferroptosis occurs through an osmotic mechanism and propagates independently of cell rupture. *Nat Cell Biol*. 2020;22(9):1042–1048. doi:10.1038/s41556-020-0565-1
15. Jiang Z, Lim SO, Yan M, et al. TYRO3 induces anti-PD-1/PD-L1 therapy resistance by limiting innate immunity and tumoral ferroptosis. *J Clin Invest*. 2021;131(8). doi:10.1172/jci139434
16. Li T, Huang HY, Qian B, et al. Interventing mitochondrial PD-L1 suppressed IFN-gamma-induced cancer stemness in hepatocellular carcinoma by sensitizing sorafenib-induced ferroptosis. *Free Radic Biol Med*. 2024;212:360–374. doi:10.1016/j.freeradbiomed.2023.12.034
17. Lei H, Li Q, Pei Z, et al. Nonferrous ferroptosis inducer manganese molybdate nanoparticles to enhance tumor immunotherapy. *Small*. 2023;19(45):e2303438. doi:10.1002/smll.202303438
18. Deng J, Zhou M, Liao T, et al. Targeting cancer cell ferroptosis to reverse immune checkpoint inhibitor therapy resistance. *Front Cell Dev Biol*. 2022;10:818453. doi:10.3389/fcell.2022.818453
19. Zhou X, Zou L, Liao H, et al. Abrogation of HnRNP L enhances anti-PD-1 therapy efficacy via diminishing PD-L1 and promoting CD8(+) T cell-mediated ferroptosis in castration-resistant prostate cancer. *Acta Pharm Sin B*. 2022;12(2):692–707. doi:10.1016/j.apsb.2021.07.016
20. Tang B, Zhu J, Wang Y, et al. Targeted xCT-mediated ferroptosis and protumoral polarization of macrophages is effective against HCC and enhances the efficacy of the anti-PD-1/L1 response. *Adv Sci*. 2023;10(2):e2203973. doi:10.1002/advs.202203973

21. Li Z, Li B, Li L, et al. The immunostimulative effect and mechanisms of a novel mouse anti-human PD-1 monoclonal antibody on Jurkat lymphocytic cells cocultured with hepatoma cells. *Onco Targets Ther*. 2020;13:12225–12241. doi:10.2147/ott.s281397
22. Song G, Luo Q, Qin J, et al. Effects of oxymatrine on proliferation and apoptosis in human hepatoma cells. *Colloids Surf B Biointerfaces*. 2006;48(1):1–5. doi:10.1016/j.colsurfb.2005.12.012
23. Li Z, Gao WQ, Wang P, et al. Pentamethylquercetin inhibits hepatocellular carcinoma progression and adipocytes-induced PD-L1 expression via IFN-gamma signaling. *Curr Cancer Drug Targets*. 2020;20(11):868–874. doi:10.2174/1568009620999200730184514
24. Dai Z, Wang L, Wang X, et al. Oxymatrine induces cell cycle arrest and apoptosis and suppresses the invasion of human glioblastoma cells through the EGFR/PI3K/Akt/mTOR signaling pathway and STAT3. *Oncol Rep*. 2018;40(2):867–876. doi:10.3892/or.2018.6512
25. Lou D, Fang Q, He Y, et al. Oxymatrine alleviates high-fat diet/streptozotocin-induced non-alcoholic fatty liver disease in C57BL/6 J mice by modulating oxidative stress, inflammation and fibrosis. *Biomed Pharmacother*. 2024;174:116491. doi:10.1016/j.biopha.2024.116491
26. Dunnigan A, Comment on: Jilkova ZM, et al. "Predictive factors for response to PD-1/PD-L1 checkpoint inhibition in the field of hepatocellular carcinoma: current status and challenges" cancers 2019, 11, 1554. *Cancers*. 2020;12(9). doi:10.3390/cancers12092670
27. He YF, Wang XH, Zhang GM, et al. Sustained low-level expression of interferon-gamma promotes tumor development: potential insights in tumor prevention and tumor immunotherapy. *Cancer Immunol Immunother*. 2005;54(9):891–897. doi:10.1007/s00262-004-0654-1
28. Xiang J, Zhang N, Sun H, et al. Disruption of SIRT7 increases the efficacy of checkpoint inhibitor via MEF2D regulation of programmed cell death 1 ligand 1 in hepatocellular carcinoma cells. *Gastroenterology*. 2020;158(3):664–678. doi:10.1053/j.gastro.2019.10.025
29. Ramadori P, Gallage S, Heikenwalder MF. Unique tumour microenvironment: when ferroptosis activation boosts ICI of liver cancer. *Gut*. 2023;72(9):1639–1641. doi:10.1136/gutjnl-2023-329472
30. Borst J, Ahrends T, Babala N, et al. CD4(+) T cell help in cancer immunology and immunotherapy. *Nat Rev Immunol*. 2018;18(10):635–647. doi:10.1038/s41577-018-0044-0
31. Ye C, Yao Z, Wang Y, et al. Asiaticoside promoted ferroptosis and suppressed immune escape in gastric cancer cells by downregulating the Wnt/beta-catenin pathway. *Int Immunopharmacol*. 2024;134:112175. doi:10.1016/j.intimp.2024.112175